Desalination and Water Treatment
www.deswater.com

doi: 10.5004/dwt.2017.20549

78 (2017) 90–97
June

Kinetics study on the adsorption/desorption process using activated carbon electrodes with single-pass mode in capacitive deionization

Ruohan Zhang, Shaojie Jiang*

Key Laboratory of Three Gorges Reservoir Region's Eco-Environment, Ministry of Education, Chongqing University, Faculty of Urban Construction and Environment Engineering, Chongqing 400045, China, Tel./Fax: +86 2365120759; emails: shaojiejiang@hotmail.com (S. Jiang), zrhcc@hotmail.com (R. Zhang)

Received 9 September 2016; Accepted 1 February 2017

ABSTRACT

Based on pseudo-first-order and pseudo-second-order equations, the kinetic study on the adsorption/desorption process of activated carbon upon various operation parameters using single-pass mode was conducted for the first time. An optimum flow rate for desorption was found, below or beyond which desorption rate could decrease due to the long retention and turbulence respectively. The adsorption rate rose with an increase of influent concentration but the increasing trend of adsorption capacity was not obvious, while desorption rate fell due to the decrease of concentration gradient between micropores and external solution. The salt ions could not penetrate into or out of the whole electrode for thick electrodes within a reasonable period. As the applied voltage increased, the adsorption capacity of activated carbon increased while both the adsorption rate and the desorption rate decreased. Kinetics analysis indicated that the adsorption/desorption process of KCl in activated carbon electrodes followed pseudo-first-order kinetics model.

Keywords: Capacitive deionization; Activated carbon; Adsorption/desorption process; Kinetics analysis

1. Introduction

Freshwater crisis has become an urgent problem not only in China but also in the whole world [1,2]. Undoubtedly, utilizing the seawater and brackish water is a feasible way to provide sustainable clear water for human beings [3]. Traditional desalination technologies, such as reverse osmosis, multistage flash, multieffect distillation and electrodialysis, have issues in maintenance, complex pre-treatment, high temperature and high energy consumption [4,5]. In contrast, capacitive deionization (CDI) with a simple operating pattern, low costs of materials and low energy requirements is a potential alternative desalination technology [6,7].

CDI technology is based on static electroadsorption. Once a potential is applied onto the carbon electrodes, which is known as charging, the salt ions migrate into the electrodes and are held in the micropores forming electrical double layers (EDLs). When the potential is removed by short circuit, which is called discharging, the adsorbed salt ions are released back into the solution making the electrode regenerate and be ready for the next desalination process [8,9].

Although CDI owns many advantages compared with traditional desalination technologies, to become available and reliable, there is a great amount of works needed to do. In recent years, material is a hot spot, including modifying the zero charge by surface treatment [10], coating metallic oxide to improve wettability [11], manufacturing new carbon materials such as mesopore carbon [12], carbon nanotube, carbon nanofibers [13] and so on. Despite the fact that these new carbon-based materials have a better performance in CDI, their manufacturing process is complicated, and the mass production is costly; therefore, the commercial activated carbon with a low price and a large specific surface area is the most suitable material for large-scale application at present [14].

* Corresponding author.

Generally, a complete cycle of CDI consists of adsorption and desorption. Most researches focus on the adsorption process. Kinetics is essential to estimate the electrosorption behavior of CDI. Pseudo-first-order and pseudo-second-order kinetic equations are the most common model that have been proposed to describe the electrosorption kinetics of CDI adsorption processes. Chen et al. [14], Park and Kwak [15] and Wang et al. [16] successfully used pseudo-first-order and pseudo-second-order kinetic equations to modeling the electrosorption of NaCl on activated carbon electrode. Also, Bian et al. [17] used pseudo-first order to analyze the adsorption process in membrane capacitive deionization. Another way to model the electrosorption kinetics of CDI is by Nernst–Planck equation. Dykstra et al. [18] and Tang et al. [19] described the electrosorption process of CDI well with Nernst–Planck equation. Meanwhile, the activated carbon electrodes with different thickness [20] or asymmetric surface area [21] have a great influence on CDI. On the other hand, much fewer researches focus on the desorption process, which actually plays a significant role in the next adsorption process. Porada et al. [9] reported reversed-voltage desorption process, during which the voltage level is changed to values opposite in magnitude to that during adsorption. It enhances the adsorption rate and total salt adsorption per cycle while problems could also be brought. Yao and Tang [22] explored the occurrence of re-adsorption that may impose a negative impact on electrode regeneration in CDI. However, to the authors' knowledge, there is no report about the kinetics study on the desorption process. Meanwhile, there is no detailed kinetic study upon different salt concentration and different electrode thickness during adsorption process in CDI with single-pass mode. Therefore, more research efforts are needed.

In this study, the adsorption/desorption performance of KCl upon various operational parameters on activated carbon has been studied. Pseudo-second-order and pseudo-second-order equations were used to model both adsorption and desorption processes, aiming to provide a better understanding of them in CDI.

2. Experiment

2.1. Fabrication of carbon electrodes

Carbon electrodes used in this paper were prepared by mixing the activated carbon powder (YP-50F), carbon black (VXC72R) and polyvinylidene fluoride (molecular weight = 53,400) dissolved in Dimethylacetamide (Dmac, 99%). The mixture was stirred for 12 h to ensure homogeneity, and then the mixed slurry was cast onto a titanium plate through a doctor blade with a thickness of 0.5 or 1 mm followed by drying at 60°C for 2 h to form a carbon electrode. To remove all organic residual remained in the micropores, the carbon electrode was further dried at 60°C in a vacuum oven for 2 h. The size of a single activated carbon electrode is 7 cm × 18 cm.

2.2. CDI cell configuration

A CDI cell consisted of a pair of electrodes that were separated by a nylon spacer (about 100 μm) to create a flow channel for water. Teflon gaskets were used to seal the cell, while two thick plastic end plates and twenty screws were utilized to hold the cell.

2.3. Capacitive deionization experiments

CDI experiments were conducted in the CDI cell(s) with a single-pass flow-by system as shown in Fig. 1. A given potential was applied to the CDI cell using a potentiostat (Maynuo, M8872). The adsorption process was conducted applying a pre-established potential. Then the desorption process was conducted through short circuit until the conductivity of effluent withdraw to the feed water. To minimize the possible influence caused by the difference of hydration radius between anion and cation, KCl was used as electrolyte solutions, which was supplied by a peristaltic pump (BT-1002J). The conductivity of the effluent passing through the CDI cell was measured automatically by a conductivity meter (Multi 3420) at intervals of 5 s (the minimal interval of the conductivity meter).

2.4. Adsorption/desorption calculation and kinetic analysis

The amount of adsorbed (desorbed) KCl per unit mass of activated carbon electrodes was calculated from Eq. (1):

$$Q_a(Q_d) = 1000\int_{t1}^{t2}\frac{(C - C_{in})v}{60000M}dt \quad (1)$$

where C (mM) and C_{in} (mM) are the effluent and influent concentration of KCl solution, respectively. M (g) is the mass of the activated carbon electrodes including cathode and anode. v (mL/min) is the flow rate.

Pseudo-first-order and pseudo-second-order are employed to fit experimental data. The form of the equations are as follows:

$$Q_a(Q_d) = Q_0(1 - e^{-k_1 t}) \quad (2)$$

$$Q_a(Q_d) = Q_o(1 - \frac{1}{1 + Q_o k_2 t}) \quad (3)$$

where k_1 (min^{-1}) is the pseudo-first-order desorption rate constant, and k_2 [g·(mmol·min)$^{-1}$] is the pseudo-first-order desorption rate constant. $Q_a(Q_d)$ (μmol/g) is the amount of adsorbed/desorbed KCl at time t (min), and Q_0 (μmol/g) is the total amount of adsorbed/desorbed KCl.

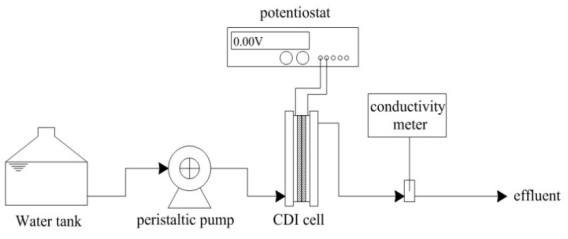

Fig. 1. Schematic diagram of CDI experiments.

3. Results and discussion

3.1. Desorption performance upon different flow rates

The influence of the flow rate on the adsorption process has been studied by many researchers while few eyes were put on the desorption process. The effect of the flow rate on desorption process was studied.

The adsorption stage of all seven experiments was the same that the CDI cell was charged at a potential of 1.2 V for 30 min at a flow rate of 16 mL/min to reach the largest adsorption capacity. Desorption was carried out by short circuit at seven different flow rates (8, 16, 24, 32, 48, 80 and 160 mL/min).

Figs. 2(a) and (b) present the concentration of effluent as a function of time during adsorption and desorption processes, respectively. The amount of KCl absorbed was 159.06 μmol for per gram of carbon electrodes when the adsorption was accomplished.

Experimental data of desorption process and kinetics fitting curves were presented in Figs. 2(c)–(i). More details were shown in Table 1. It revealed that pseudo-first-order kinetics equation could fit the experimental data better than pseudo-second-order kinetics equation due to the higher value of the correlation coefficient (R^2), indicating that the desorption process followed pseudo-first-order kinetics. At the flow rates ranging from 8 to 32 mL/min, the desorption rate went up with an increase of the flow rate suggesting that the adsorbed ions desorbed faster as the increase of the flow rate. At the flow rate of 8 mL/min, the retention time of the salt ions released from the carbon electrodes was longer than others, which hindered the further desorption process, resulting in slowest desorption rate. With an increase of the flow rate, the salt ions released from carbon electrodes was able to be carried out from the CDI cell sooner benefiting the desorption process. While the flow rate increased continuously (48, 80 and 160 mL/min), desorption rate decreased indicating

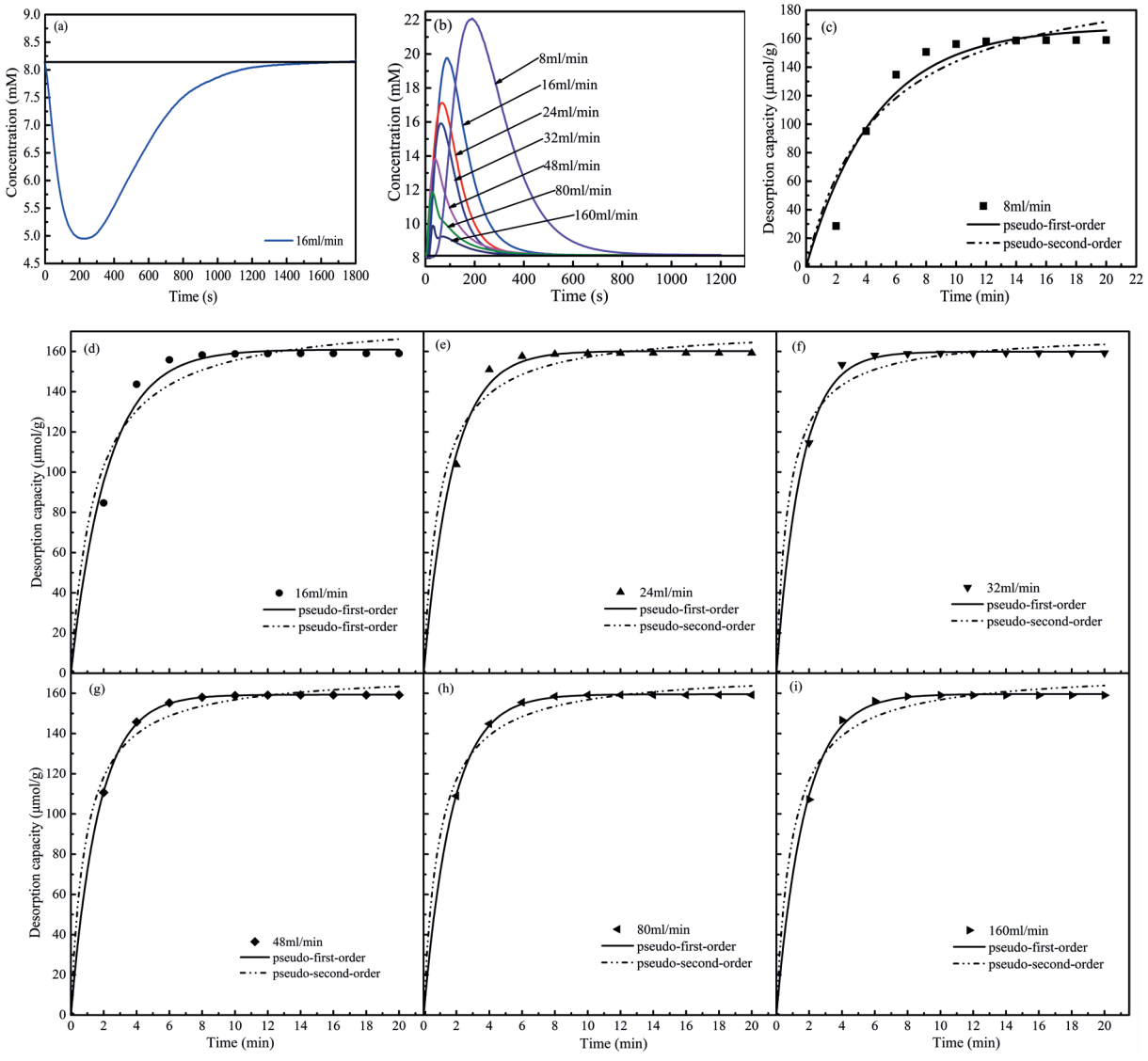

Fig. 2. (a) Concentration change of effluent during adsorption process; (b) concentration change of effluent at different flow rate during desorption process; and (c)–(i) desorption performance and kinetics fitting curves using different carbon electrodes.

that the turbulence caused by the high flow rate could also limit desorption of the salt ions. In our study, the desorption rate reached the highest level at the flow rate of 32 mL/min.

Table 1
The desorption parameters of pseudo-first-order and pseudo-second-order kinetics for KCl with different desorption flow rates

r	Pseudo-first-order			Pseudo-second-order		
	Q_0	$k_1 \times 10^{-1}$	R^2	Q_0	$k_2 \times 10^{-3}$	R^2
8	167.95	2.16	0.9531	213.01	0.98	0.9264
16	160.95	4.49	0.9888	178.34	3.83	0.9631
24	160.21	5.70	0.9958	172.40	6.02	0.9778
32	159.89	6.62	0.9983	169.52	8.04	0.9857
48	159.33	6.00	0.9999	170.69	6.63	0.9905
80	159.54	5.82	0.9999	171.36	6.29	0.9894
160	159.67	5.78	0.9992	171.61	6.20	0.9861

3.2. Adsorption/desorption performance upon different influent concentration

Concentration has a significant impact on the adsorption performance of CDI as well as the desorption process. KCl solution with three concentrations (8, 12 and 16 mM) was used as the feed water in this paper. During the adsorption stage, the cell was charged upon a potential of 1.2 V for 30 min at a flow rate of 16 mL/min to reach the largest adsorption capacity and then entered into the desorption stage.

Fig. 3(a) shows experimental data of the effluent as a function of time with different concentrations (8, 12 and 6 mM). The adsorption capacity was 159.06, 161.19 and 162.44 μmol/g for 8, 12 and 16 mM, respectively, after the adsorption stage. The amount of KCl absorbed did not increase as much as the concentration increased. In a batch-mode experiment, the amount of adsorbed ions would notably increased as increase of the concentration [23]. Unlike batch-mode experiments, the concentration of influent is constant in the single-pass

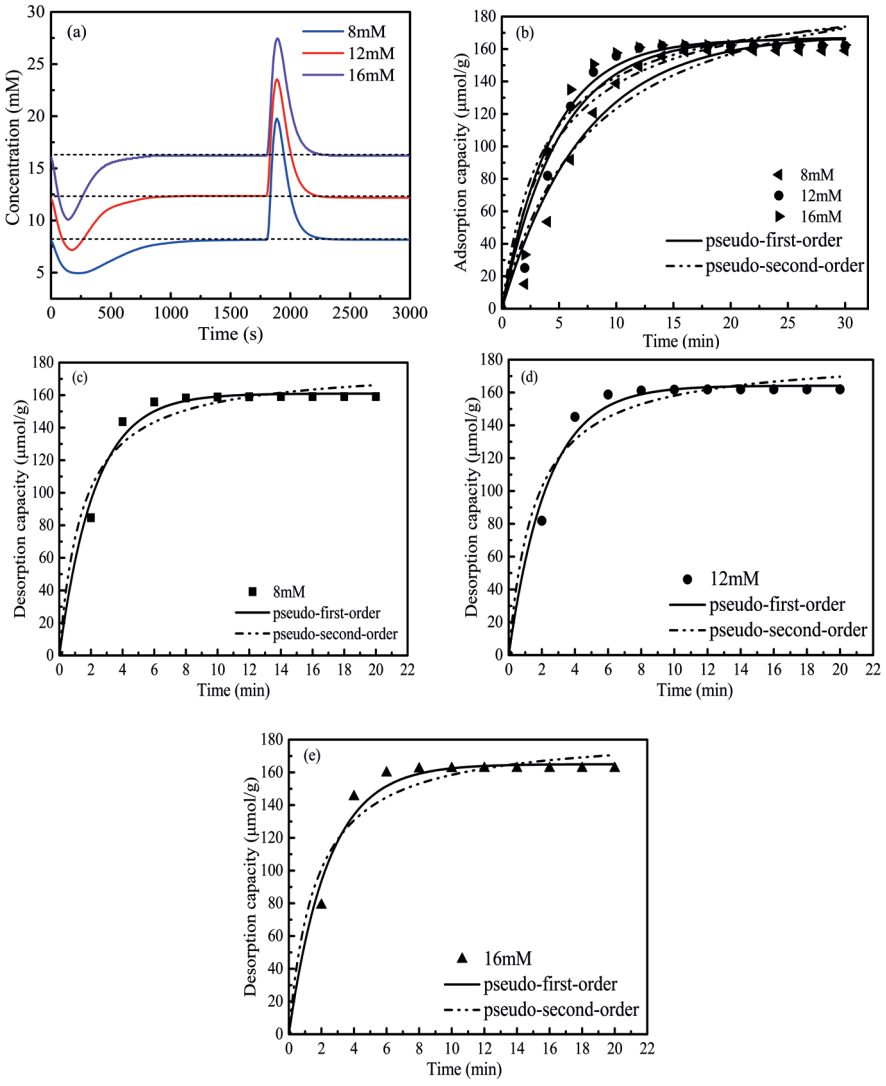

Fig. 3. (a) Concentration change of effluent upon different influent concentration; (b) adsorption performance and kinetics fitting curves of different influent concentration; and (c)–(e) desorption performance and kinetics fitting curves of different influent concentration.

mode so the carbon electrodes are much easier to reach their largest adsorption capacity. In the work of Kim et al. [24], the adsorption capacity of carbon electrodes using 5, 20 and 80 mM NaCl solution was nearly unchanged.

Figs. 3(b)–(d) display both the experimental data and fitting curves using pseudo-first-order and pseudo-second-order kinetics equation. More details are shown in Tables 2 and 3. It was found that pseudo-first-order kinetics equation could fit the experimental data better than pseudo-second-order kinetics equation indicating that the adsorption and desorption processes followed pseudo-first-order kinetics. With the increase of influent concentration, the adsorption rate increased while the desorption rate decreased. It could be attributed to the decrease of concenration gradient between micropores and external solution, since the amout of KCl absorbed was nearly the same whlist the concetration of influent increased, making the desorption rate slower.

3.3. Adsorption/desorption performance upon different electrode thickness

The electrode thickness has a great influence on CDI. In the work of Porada et al. [20], despite the fact that the electrode thickness varied, what actually matters was the cathode/anode mass ratio. In this study, three types of electrodes were used: type 1: electrodes of 0.5 mm casting thick, about 3 g; type 2: electrodes of 0.5 mm casting thick, about 6 g; type 3: electrodes of 1 mm casting thick, about 6 g. The electrodes mass is the sum of anode and cathode, so type 1 and type 3 had one CDI cell while type 2 had two cells. A potential of 1.2 V was applied until the carbon electrode reached the largest adsorption capacity and then removed by short circuit. The flow rate was maintained at 16 mL/min.

The change of concentration of effluent using different electrodes is shown in Fig. 4(a). The adsorption capacity of types 1, 2 and 3 was 159.06, 159.07 and 157.07 μmol/g, respectively. It indicated that all carbon electrodes became saturated after adsorption. The lowest concentration of effluent using type 3 in the adsorption process was 5.72 mM, which was higher than type 1 (4.95 mM) and type 2 (2.99 mM), suggesting that the thick electrodes limited the adsorption process.

Experimental data and fitting curves are displayed in Figs. 4(b) and (c). More details are presented in Tables 4 and 5. It was found that pseudo-first-order kinetics equation could fit the experimental data better than pseudo-second-order kinetics equation due to the higher value of the correlation coefficient (R^2), indicating that the adsorption and desorption processes followed pseudo-first-order kinetics. Compared with type 1 and type 2, the adsorption rate of type 3 decreased by 66% and 49%, respectively, also revealing that increasing thickness of electrodes made the adsorption process become harder. Compared with type 1, the adsorption rate of type

Table 2
The adsorption parameters of pseudo-first-order and pseudo-second-order kinetics using different influent concentration

C_{in}	Pseudo-first-order			Pseudo-second-order		
	Q_0	$k_1 \times 10^{-1}$	R^2	Q_0	$k_2 \times 10^{-3}$	R^2
8	168.93	1.40	0.9595	216.19	0.61	0.9329
12	167.06	2.01	0.9597	199.48	1.13	0.9218
16	166.18	2.31	0.9668	193.63	1.45	0.9278

Table 3
The desorption parameters of pseudo-first-order and pseudo-second-order kinetics using different influent concentration

C_{in}	Pseudo-first-order			Pseudo-second-order		
	Q_0	$k_1 \times 10^{-1}$	R^2	Q_0	$k_2 \times 10^{-3}$	R^2
8	160.95	4.49	0.9888	178.34	3.83	0.9631
12	164.14	4.31	0.98546	182.99	3.47	0.9576
16	165.00	4.18	0.98215	184.75	3.27	0.9524

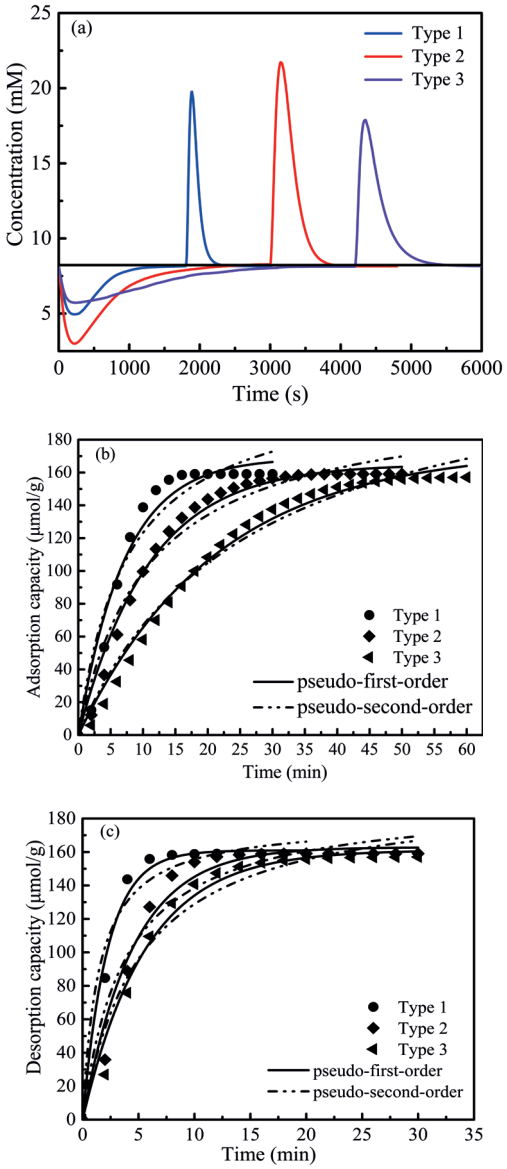

Fig. 4. (a) Concentration change of effluent using different carbon electrodes; (b) adsorption performance and kinetics fitting curves using different carbon electrodes; and (c) desorption performance and kinetics fitting curves using different carbon electrodes.

Table 4
The adsorption parameters of pseudo-first-order and pseudo-second-order kinetics using different carbon electrodes

Type	Pseudo-first-order			Pseudo-second-order		
	Q_0	$k_1 \times 10^{-1}$	R^2	Q_0	$k_2 \times 10^{-3}$	R^2
1	168.93	1.40	0.9595	216.19	0.61	0.9329
2	165.11	0.92	0.9864	206.40	0.45	0.9656
3	174.29	0.47	0.9881	241.54	0.16	0.9784

Table 5
The desorption parameters of pseudo-first-order and pseudo-second-order kinetics using different carbon electrodes

Type	Pseudo-first-order			Pseudo-second-order		
	Q_0	$k_1 \times 10^{-1}$	R^2	Q_0	$k_2 \times 10^{-3}$	R^2
1	160.95	4.49	0.9888	178.34	3.83	0.9631
2	162.85	2.22	0.9736	190.70	1.39	0.9372
3	161.12	1.78	0.9802	195.73	0.98	0.9543

2 decreased by 34% due to two cells of type 2. The influent concentration of the later cell was below 8 mM until the former cell became saturated and resulted in a slower adsorption rate. For the same consequence, the influent concentration of the later cell was beyond 8 mM until the former cell completely regenerated leading to a slower desorption rate. Compared with types 1 and 2, the desorption rate of type 3 decreased by 60% and 13%, respectively. The salt ions could not penetrate into or out of activated carbon electrodes in a reasonable period of time for thick electrodes, resulting in a slower adsorption/desorption rate.

3.4. Adsorption/desorption performance upon various applied voltage

Applied voltage is a vital parameter in CDI. Considering that the amount of KCl absorbed may be too low at a low applied voltage (0.3 V), which could bring obstacles for measurement and calculation; we used carbon electrodes of type 2. During the adsorption stage, the cells were charged upon different potential for 50 min at a flow rate of 16 mL/min and then entered into desorption through short circuit.

Fig. 5(a) shows experimental data of the effluent at different applied voltages. The adsorption capacity was 11.97, 50.29, 111.85 and 159.07 μmol/g for 0.3, 0.6, 0.9 and 1.2 V, respectively. The amount of adsorbed KCl increased as the applied voltage increased. The higher applied potential would build the thicker electric double layer, and the salt ions were able to migrate into the deeper space of micropores, increasing the ability of desalination.

Experimental data and fitting curves are displayed in Figs. 5(b) and (c). More details are presented in Tables 6 and 7. It was found that pseudo-first-order kinetics equation could fit the experimental data better than pseudo-second-order kinetics equation due to the higher value of the correlation coefficient (R^2), indicating that the adsorption and desorption processes followed pseudo-first-order kinetics. With the increase of applied voltage, the desorption rate decreased indicating that more KCl absorbed in the adsorption process

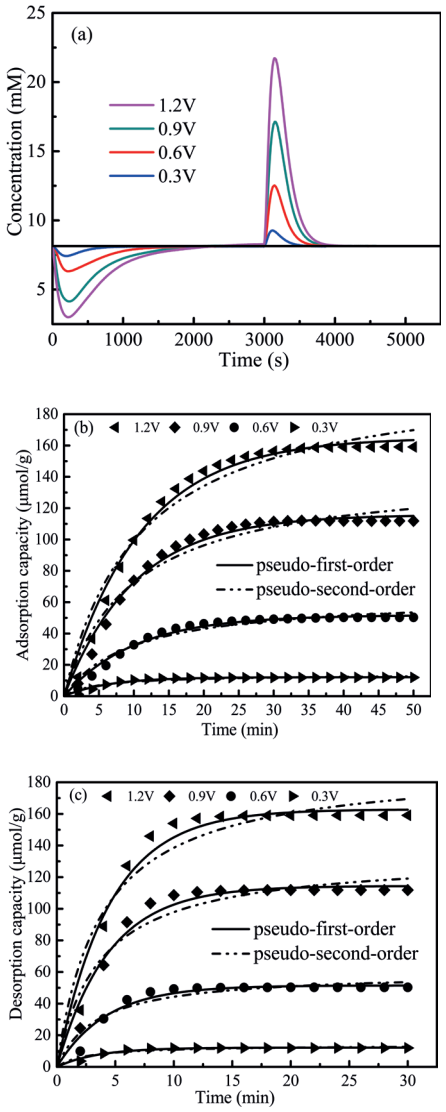

Fig. 5. Concentration change of effluent at various applied voltage; (b) adsorption performance and kinetics fitting curves using different carbon electrodes; (c) desorption performance and kinetics fitting curves using different carbon electrodes.

resulted in a slower desorption rate. Besides, more salt ions were able to migrate into the deeper space of micropores that have complex and irregular pore structure, leading to the decrease of the desorption rate.

The adsorption process was a bit complicated. With the increase of applied voltage, the salt ions have the ability to migrate into electrodes faster due to stronger electric force while the adsorption capacity also increased, which had a negative impact on the adsorption rate. It seemed that these two processes reached equilibrium at the applied voltages of 0.6 and 0.9 V due to the same adsorption rate constant (0.99×10^{-1} min^{-1}). Compared with the adsorption rate at 0.3 V, the adsorption rate of 1.2 V decreased by 41%, which was contrary to the results of Chen et al. [14], in which the adsorption rate at 1.2 V was the fastest using 8.55 mM NaCl solution. This contrary could be attributed to the influence of the plate distance. The smaller plate distance could shorten the migration

Table 6
The adsorption parameters of pseudo-first-order and pseudo-second-order kinetics for KCl upon various applied voltages

V	Pseudo-first-order			Pseudo-second-order		
	Q_0	$k_1 \times 10^{-1}$	R^2	Q_0	$k_2 \times 10^{-3}$	R^2
0.3	12.10	1.57	0.9727	13.91	14.32	0.9326
0.6	51.76	0.99	0.9858	63.85	1.62	0.9630
0.9	115.87	0.99	0.9835	142.98	0.72	0.9589
1.2	165.11	0.92	0.9864	206.41	0.15	0.9656

Table 7
The desorption parameters of pseudo-first-order and pseudo-second-order kinetics for KCl upon various applied voltages

V	Pseudo-first-order			Pseudo-second-order		
	Q_0	$k_1 \times 10^{-1}$	R^2	Q_0	$k_2 \times 10^{-3}$	R^2
0.3	12.16	2.84	0.9762	13.74	27.99	0.9358
0.6	51.44	2.35	0.9617	59.85	4.77	0.9209
0.9	114.42	2.26	0.9706	133.59	2.05	0.9328
1.2	162.85	2.22	0.9736	190.70	1.39	0.9372

distance that would benefit for faster formation of the electric double layer; meanwhile, the smaller distance could lower resistance [25], suggesting that applied voltage would have greater influence on adsorption process with the increase of plate distance. In Chen's work [14], the plate distance was 4 mm, making the desalination performance more sensitive to the variation of applied voltage. In our study, the cathode and anode were separated by a nylon spacer with a thickness of only about 100 μm, which enormously decreased the time of ion movement from spacer to carbon electrodes and the solution resistance caused by plate distance, minimizing the influence of plate distance on adsorption performance.

As Fig. 5(a) displays, the concentration of effluent at 0.3 V was steadier than others, indicating steadier solution concentration between cathode and anode during adsorption process could contribute to faster adsorption. Besides, more salt ions were able to migrate into the deeper space of micropores that have complex and irregular pore structure, resulting in a decrease of the adsorption rate.

4. Conclusions

The adsorption/desorption performance and kinetics upon various operating parameters of activated carbon in CDI were investigated. It was found that there was an optimum flow rate for desorption. The long retention of water flow at a slow flow rate and turbulence caused by a high flow rate hindered the desorption process of adsorbed salt ions. With an increase of influent concentration, the decrease of concentration gradient between micropores and external solution hinderd the desorption process. As the electrode thickness increased, it was harder for the salt ions to penetrate into or out of carbon electrode for thick electrodes, which led to a slower adsorption or desorption rate, suggesting that with the same mass materials, thinner carbon electrodes would be a better choice. And when the applied voltage increased, compared with the stronger electric force, the increase of the adsorption capacity has a greater impact on the adsorption rate, leading to a slower adsorption rate. Meanwhile, the more KCl was adsorbed, the slower desorption rate was. The results showed that the adsorption/desorption process of CDI with single-pass mode followed pseudo-first-order kinetics model.

References

[1] F. Duan, Y. Li, H. Cao, Y. Wang, J.C. Crittenden, Y. Zhang, Activated carbon electrodes: electrochemical oxidation coupled with desalination for wastewater treatment, Chemosphere, 125 (2015) 205–211.
[2] Q. Zaib, H. Fath, Application of carbon nano-materials in desalination processes, Desal. Wat. Treat., 51 (2013) 627–636.
[3] Z. Chen, H. Zhang, C. Wu, Y. Wang, W. Li, A study of electrosorption selectivity of anions by activated carbon electrodes in capacitive deionization, Desalination, 369 (2015) 46–50.
[4] F.A. AlMarzooqi, A.A. Al Ghaferi, I. Saadat, N. Hilal, Application of capacitive deionisation in water desalination: a review, Desalination, 342 (2014) 3–15.
[5] Y. Wimalasiri, L. Zou, Carbon nanotube/graphene composite for enhanced capacitive deionization performance, Carbon, 59 (2013) 464–471.
[6] T.J. Welgemoed, C.F. Schutte, Capacitive deionization technology™: an alternative desalination solution, Desalination, 183 (2005) 327–340.
[7] E. Garcia-Quismondo, C. Santos, J. Lado, J. Palma, M.A. Anderson, Optimizing the energy efficiency of capacitive deionization reactors working under real-world conditions, Environ. Sci. Technol., 47 (2013) 11866–11872.
[8] A. Subramani, J.G. Jacangelo, Emerging desalination technologies for water treatment: a critical review, Water Res., 75 (2015) 164–187.
[9] S. Porada, R. Zhao, A. van der Wal, V. Presser, P.M. Biesheuvel, Review on the science and technology of water desalination by capacitive deionization, Prog. Mater. Sci., 58 (2013) 1388–1442.
[10] T. Wu, G. Wang, F. Zhan, Q. Dong, Q. Ren, J. Wang, J. Qiu, Surface-treated carbon electrodes with modified potential of zero charge for capacitive deionization, Water Res., 93 (2016) 30–37.
[11] C. Kim, J. Lee, S. Kim, J. Yoon, TiO_2 sol–gel spray method for carbon electrode fabrication to enhance desalination efficiency of capacitive deionization, Desalination, 342 (2014) 70–74.
[12] L. Zou, L. Li, H. Song, G. Morris, Using mesoporous carbon electrodes for brackish water desalination, Water Res., 42 (2008) 2340–2348.
[13] X.Z. Wang, M.G. Li, Y.W. Chen, R.M. Cheng, S.M. Huang, L.K. Pan, Z. Sun, Electrosorption of NaCl solutions with carbon nanotubes and nanofibers composite film electrodes, Electrochem. Solid-State Lett., 9 (2006) E23–E26.
[14] Z. Chen, C. Song, X. Sun, H. Guo, G. Zhu, Kinetic and isotherm studies on the electrosorption of NaCl from aqueous solutions by activated carbon electrodes, Desalination, 267 (2011) 239–243.
[15] K.-H. Park, D.-H. Kwak, Electrosorption and electrochemical properties of activated-carbon sheet electrode for capacitive deionization, J. Electroanal. Chem., 732 (2014) 66–73.
[16] G. Wang, B. Qian, Q. Dong, J. Yang, Z. Zhao, J. Qiu, Highly mesoporous activated carbon electrode for capacitive deionization, Sep. Purif. Technol., 103 (2013) 216–221.
[17] Y. Bian, P. Liang, X. Yang, Y. Jiang, C. Zhang, X. Huang, Using activated carbon fiber separators to enhance the desalination rate of membrane capacitive deionization, Desalination, 381 (2016) 95–99.
[18] J.E. Dykstra, R. Zhao, P.M. Biesheuvel, A. van der Wal, Resistance identification and rational process design in Capacitive Deionization, Water Res., 88 (2016) 358–370.
[19] W. Tang, P. Kovalsky, B. Cao, T.D. Waite, Investigation of fluoride removal from low-salinity groundwater by single-pass constant-voltage capacitive deionization, Water Res., 99 (2016) 112–121.

[20] S. Porada, M. Bryjak, A. van der Wal, P.M. Biesheuvel, Effect of electrode thickness variation on operation of capacitive deionization, Electrochim. Acta, 75 (2012) 148–156.
[21] M. Li, Y. Chen, Z.-H. Huang, F. Kang, Asymmetric electrodes constructed with PAN-based activated carbon fiber in capacitive deionization, J. Nanomater., 2014 (2014) 1–6.
[22] Q. Yao, H.L. Tang, Occurrence of re-adsorption in desorption cycles of capacitive deionization, J. Ind. Eng. Chem., 34 (2016) 180–185.
[23] Y. Zhao, X.-m. Hu, B.-h. Jiang, L. Li, Optimization of the operational parameters for desalination with response surface methodology during a capacitive deionization process, Desalination, 336 (2014) 64–71.
[24] T. Kim, J.E. Dykstra, S. Porada, A. van der Wal, J. Yoon, P.M. Biesheuvel, Enhanced charge efficiency and reduced energy use in capacitive deionization by increasing the discharge voltage, J Colloid Interface Sci., 446 (2015) 317–326.
[25] C. Wang, H. Song, Q. Zhang, B. Wang, A. Li, Parameter optimization based on capacitive deionization for highly efficient desalination of domestic wastewater biotreated effluent and the fouled electrode regeneration, Desalination, 365 (2015) 407–415.